Desalination and Water Treatment
www.deswater.com

doi:10.5004/dwt.2018.22135

107 (2018) 305–315
March

Al-Fe exchanged natural clay as an efficient reusable catalyst for dye removal and real textile effluent treatment

Fadhila Ayari*, Selma Khelifi, Malika Trabelsi-Ayadi

Laboratoire des Applications de la Chimie aux Ressources et Substances Naturelles et à l'Environnement (LACReSNE), Université de Carthage, Faculté de Sciences de Bizerte, Zarzouna 7021, Tunisia, Tel. +21621791747, email: fadhilaayari@yahoo.fr (F. Ayari), selma.khelifi@gmail.com (S. Khelifi), malikatrabelsi_ayadi@yahoo.fr (M. Trabelsi-Ayadi)

Received 4 October 2017; Accepted 1 March 2018

ABSTRACT

The Fenton and photochemically stimulated Fenton (photo-Fenton) responses are essential because these are especially powerful for the deterioration of carcinogenic and toxic compounds in the aqueous environment utilizing heterogeneous catalysts. The reason of the current investigation was to examine the effectiveness of hydroxyl FeAl-intercalated bentonites (FeAl-bent) in Fenton and photo-Fenton techniques. Specifically, Fe/Al ratios were of interest as a mean to vary the catalytic activity. Intercalation was accomplished by means of a particle ion-exchange technique and Congo red (CR) was the model compound for degradation by hydrogen peroxide (H_2O_2) in Fenton and photo-Fenton processes using FeAl-bentonite. Also, the degradation of a real textile effluent was done under UV light irradiation. The studied catalysts were characterized by powder X-ray diffraction, N_2 adsorption/desorption, X-ray fluorescence spectroscopy, transmission electron microscopy (TEM), and ultraviolet-visible spectroscopy. The catalytic performance of pillared clay was evaluated by means of different experimental conditions, such as the Fe/Al molar ratio of the intercalating solution, the catalyst amount, the hydrogen peroxide concentration, and the pH. The treatment by Fenton process demonstrated that 50% degradation efficiency of Congo red dye was achieved after 240 min of reaction. But, in photo-Fenton process 100% degradation was accomplished after just 60 min. Moreover, pillared clay showed a high catalytic activity both for the mineralization of CR and real textile effluent and also a high stability.

Keywords: Congo red; Degradation; Fenton process; Mixed pillared bentonite; Real textile effluent; Photo-Fenton process

1. Introduction

Water pollution is a noteworthy environmental problem because of the discharge of poisonous textile dyes [1]. These colored compounds have a negative effect on aquatic environment both by blocking of mild penetration or direct destruction of aquatic animals and plants due to associated noxiousness [2]. To locate a powerful and durable answer for the exclusion of those aquatic harmful compounds, a number of treatment technologies had been examined such as ozonation [3], adsorption [4], biological process [5], reverse osmosis process [6], precipitation and flocculation [7]. However, the application of these treatment strategies has been restrained because of excessive-power consumptions or high amounts of artificial resins and chemical substances [8]. Therefore, pollutant turned into another form, and just transferred from one phase to some other phases, which required similarly treatment and disposal.

Nowadays, the advanced oxidation process keeps the outstanding attention for post-treatment of treated wastewater because of a huge amount of residuals of refractory to biodegradable organics in the wastewater [9,10].

Among these AOPs, Fenton reactions, which depend on the hydroxyl radicals ($HO^{\cdot}$) through the reaction of hydrogen peroxide (H_2O_2) and ferrous ion (Fe^{2+}), were given devel-

*Corresponding author.

1944-3994 / 1944-3986 © 2018 Desalination Publications. All rights reserved.

oping interests for wastewater treatment [11,12]. However, this homogenous Fenton reaction is associated with many significant disadvantages such as requirement of low pH range (2–3), generation of large amount of iron sludge [13], deactivation of iron ion due to its ability of complex formation with organic intermediates, requirement of neutralization before final discharge [14] and also is less appropriate since it leads to high metal (iron or other transition metal) concentrations in the final effluent. Therefore, it is necessary to resolve these problems and suggest efficient solutions.

Based on the Fenton-like reactions, various types of techniques, consisting of heterogeneous Fenton-like treatment and photo-assisted Fenton reaction had been applied to the treatment of various hazardous organic compounds [10,15] because of smooth operation, very good effect, and no discharge of secondary pollution to the surroundings. For this reason, several solids had been used as heterogeneous catalysts such as iron oxide mineral [16], clay supported Fenton catalysts [17]. Indeed, micro pore volume and specific surface area of iron-modified clay improved remarkably compared to raw clay. For this reason, modified clays show high catalytic activity with hydrogen peroxide [18,19]. Additionally, the incorporated iron species has a less toxic effect [20]. Also, the Photo Fenton process involves the in situ production of hydroxyl radicals, which is characterized by the non-selectivity in their attack. Hydroxyl radicals have a very high oxidizing power (2.8 V) next only to fluorine, and can mineralize most of the organic dyes to CO_2 and H_2O.

Fenton's process using pillared clay has proved to be promising, efficient, cost effective and an attractive treatment method for the effective degradation of dyes and hazardous organic pollutants [21]. The advantages of this process are that it is simple, easy to operate, and the reactions can be carried out under laboratory conditions. Also, this process over other oxidation processes has the advantage that there agents are easily available, cheap and cost effective.

Azo dyes are not biodegradable by aerobic treatment process [22]. However, under anaerobic conditions azo dyes can be decolorized [23] by reducing the azo bond to the potentially carcinogenic substances (e.g. amines). Therefore, its mineralization by this simple Fenton like process is important.

According to these considerations, the present study overcomes such disadvantages by means of being a process that is adequate to application in industry from cost, efficiency and time point of view. It was mentioned the guidance and characterization of the heterogeneous catalyst FeAl-bent synthesized by means of the pillaring technique of natural Tunisian clay utilized in heterogeneous Fenton and photo-Fenton processes to degrade the Congo red dye. In order to estimate the catalytic activity of these modified bentonites in distinct conditions, it was assessed various parameters affecting the catalytic performance of FeAl-bent catalysts in water treatment. The effect of H_2O_2 concentrations (10, 20, 48.5 mM), catalyst load (0.05, 0.1, 1.5 g/100 ml), initial pH of the dye solution (3,8,10) and Fe/Al molar ratio (0.01, 0.05, 0.1, 1) on the dye degradation treatment. In addition, activity and stability of these materials were assessed on the photo-Fenton degradation of Congo red aqueous solutions through H_2O_2 under ultraviolet irradiation at room temperature.

2. Experimental

2.1. Chemicals and materials

Parental clay employed in this work, gathered from soils of Tboursouk (North-West of Tunisia), was prepared and purified as defined in another research work [24] .

The Al-Fe-bent surface area and cation exchange capacity (CEC) were 504 m^2/g and 71.93 meq/100 g. The chemical composition is (19.05% Al_2O_3, 52.04% SiO_2, 6.81% Fe_2O_3, 2.24% MgO, 0.14% CaO, 1.50% Na_2O, 0.95% K_2O) and the structural formula is $Ca_{0.22}Na_{0.422}K_{0.174}(Si_{7.58}Al_{0.42})(Al_{2.86}Fe_{0.748}Mg_{0.48})O_{22}$.

The anionic dye, Congo red (CR),was obtained from Sigma Chemical, as model of a secondary diazo dye. It was used without further purification, it is a secondary diazo dye.

All solutions and dispersions were prepared using deionized water.

All chemicals as $AlCl_3{\cdot}6H_2O$, $FeCl_3{\cdot}6H_2O$, Na_2CO_3, H_2O_2 (35%, w/w), NaOH and HCl, were purchased from commercial sources as guaranteed-grade reagents and used without further purification.

2.2. Catalysts preparation

Fe/Al-pillared bentonites were synthesized through the reaction of Na-bentonite with base-hydrolyzed solutions of Fe and Al via cation exchange process. The synthesized procedure was carried out according to the following method: An intercalate solution was prepared by titration of an Al^{3+}/Fe^{3+}cationic solution (i.e. 0.18 M $AlCl_3{\cdot}6H_2O$ and 0.02 M $FeCl_3{\cdot}6H_2O$) with 0.2 M NaOH. The addition of NaOH to the cationic solution was attempted under stirring at a controlled speed rate and 70°C for 12 h. These pillaring solutions containing Fe-polyhydroxy and Al-polyhydroxy species were aged for 7 d at room temperature before use.

Pillared bentonites were prepared by drop wise adding drop wise of the pillaring solution to a 2% suspension of Na-bentonite under stirring corresponding to a metal/Na-bent ratio of 3.8. The suspension was aged for 1 d at room temperature. Then, the resulting dispersion was left for 24 h and the supernatant excess was eliminated. The sediment was dialyzed with distilled water until chloride was absent. After that, the pillared clay was dried at 80°C and calcined at 500°C for 2 h [24].

The samples obtained with a Fe/Al molar ratio of 0.01, 0.05, 0.1, and 1 are denoted below as $FeAl_{0.01}$-bent, $FeAl_{0.05}$-bent, $FeAl_{0.1}$- bent and $FeAl_1$- bent, respectively.

2.3. Catalysts characterization

The chemical composition of the pillared bentonites was determined by X-ray fluorescence using a commercial instrument(ARL 9900 of Thermo Fisher), using monochromatic radiation Kα1of Cobalt (λ = 1.788996 Å).

X-ray diffraction analysis of heterogeneous catalysts was investigated using a PAN alytical X' Pert High Score plus diffractometer, CuKα radiation and 2θ from 2 to 15°. X-ray diffraction spectra were recorded for samples dried at room temperature. Samples were analyzed as oriented clay aggregate specimens prepared by drying clay suspensions on glass slides.

BET surface area and pore volumes of catalysts were measured using the physical adsorption of nitrogen by Quantachrome model Nova 1200e analyzer of solid particles surface and porosity. Prior to the measurement, samples were out gassed at a temperature of 200°C under high vaccum for2 h. Specific surface area S_{BET} values were calculated with $0.05 < P/P_0 < 0.30$. The total pore volume (V_t) was estimated from the adsorption data at a P/P_0 value of □ 0.99. The Barrett-Joyner-Halenda (BJH) method was applied to the desorption data for P/P_0 values above 0.20 to determine the mesopore surface area S_{BJH} and themesopore volume (V_{BJH}) for pores in the 10–500 Å range. The mesopore volume distribution as a function of pore size was calculated by (BJH) method. The micropore volumes (V_{micr}) and external surface area (S_{ext}) were calculated by means of the t-plot method.

The optical properties of the studied materials were investigated by means of UV-vis diffuse reflectance spectroscopy (DRS) using UV-visible spectrophotometer (Shimadzu UV-2700). Time-resolved photoluminescence (PL) was performed on a FLS980 Spectrometer by applying laser excitation at 400 nm. Transmission electron microscopy (TEM) was utilized to determine the morphology structure of Na-bent and $FeAl_{0.1}$-bent.

2.4. Experimental system and procedure

2.4.1. Fenton oxidation of dye solution

Fenton experiments were achieved under mild conditions (atmospheric pressure and 25°C) using Congo red as model pollutant and H_2O_2 as oxidant. The pH value of dye solution was adjusted before the oxidation attempted. Reaction began by adding in 100 ml of $5{\cdot}10^{-4}$ M Congo red solution of the required quantity of catalyst and stirring in the dark until the adsorption-desorption equilibrium was achieved before the initiation of oxidation. Then, the desired amount of $H_2O_2$was added to the reaction solution to start the oxidation. The concentration of hydrogen peroxide was varied in multiples of stoichiometry amount,which is theoretically required to completely oxidize Congo red dye into CO_2, H_2O and mineral acids. The stoichiometry amount of H_2O_2 was 97 M [according to Eq. (1)] for 1 M of Congo red solution.

$$C_{32}H_{22}N_6Na_2O_6S_2 + 97\ H_2O_2 \rightarrow 32CO_2 + 104H_2O + 6NO_3^- + 2SO_4^{2-} + 2Na^+ + 8H^+ \quad (1)$$

According to Eq. (1), the total mineralization of 1 M CR dye leads to 6 M of NO_3^- and 2M of SO_4^{2-}. Thus, for $5{\cdot}10^{-4}$ M of CR dye a $30{\cdot}10^{-4}$ M $NO_3^-$and $10{\cdot}10^{-4}$ MSO_4^{2-}were obtained.

The overall reaction time was fixed at 240 min. In addition, there are numbers of experimental conditions affecting on the rate and performance of catalytic system, a set of smart experiments was carried out to optimize the catalytic system. Initial molar concentrations of H_2O_2 (10, 20, and48.5 mM), catalyst loading (0.05, 0.1, and 1.5 g/100 ml) and initial pH of solution (3, 8, and 11) were investigated.

At different time intervals, samples were taken out by syringe and mixed with KI to eliminate residual hydrogen peroxide, and the catalyst was separated from the solution by centrifugation. The supernatant was filtered via a 0.45 µm filter membrane and then used to evaluate the dye degradation /mineralization.

The percent of Congo red degradation was calculated taking into account the initial adsorption phase on the catalyst surface:

$$\text{Degradation (\%)} = (C_0 - C_t)/C_0 \times 100$$

where C_t is the dye concentration at time t (min) and C_0 is the initial concentration after adsorption-desorption equilibrium.

2.4.2. Oxidation and photo-Fenton oxidation of dye solution

The photo catalytic activities of as-synthesized heterogeneous catalysts were investigated by photo degradation of 150 ml Congo red aqueous solution with $5{\cdot}10^{-4}$ M concentration at neutral pH. The suspension was set apart with magnetic stirring at room temperature and dark conditions for 40 min to achieve the adsorption-desorption equilibrium. Next, desired amount of hydrogen peroxide was introduced in the solution and the suspension was exposed to UV-visible light irradiations for 90 min. Irradiation was provided by a 125 W Philips HPK UV-lamp (UV-A) placed in a plugging tube. A Pyrex cylindrical jacket located around the plugging tube allows an irradiation with wavelengths of around $\lambda = 350$ nm.

At given intervals of reaction, 3 ml of the suspension were taken for analysis, centrifuged to remove the photo catalyst and filtered through a 0.45 µm filter membrane in the absence of light.

2.4.3. Analytical methods

The discoloration (%) in solution was determined by UV-vis spectrophotometer (Shimadzu Model Perkin Elmer), absorbance measurements were performed at the maximum wavelength of CR, meaning at 498 nm in neutral medium and at 564 nm in acidic medium.

The residual dye concentration in each experiment was performed by High Performance Liquid Chromatography (HPLC) (YL9100 HPLC System) with UV-vis spectrophotometer detector. The data was recorded by Clarity software. The column was of C_{18} type (250 mm × 4.6 mm, 5 µm). The mobile phase was 60% acetonitrile and 40% ultra pure water at a flow rate of 1 mL/min. The injection volume was 20 µL.

Ion chromatography of all samples was also conducted for confirmation of the mineralization as well as to measure the concentrations of inorganic ions. The NO_3^- and SO_4^{2-} concentrations were determined with a metrosep A Supp 4 anionic column at 40°C using a mobile phase composed of 1.8 mM Na_2CO_3 and 1.7 mM $NaHCO_3$ at 1 $mL{\cdot}min^{-1}$.

The $Fe^{}$ ions leaching from the catalyst in-time were measured using an A300 Perkin Elmer atomic absorption spectrophotometer.

For real textile effluent characterization before and after treatment, some techniques were used such as: conductivity was performed using a Tacussel model 123 conductometer;

pH measurement was determined by TW 330 pH meter;- Suspended matter (SM) in the water was gravimetric-ally quantified by filtering and drying at 105°C for 2 h. Chemicals oxygen demand (COD) was measured according to the standard titration method followed in the SARTEX Company. Also, biochemical oxygen demand (BOD_5) was investigated electrochemically by a dilution method wherein blocking nitrification was added and incubated for 5 or 7 d. Total organic carbon (TOC) analyses were performed on a multi N/C 2100 TOC analyzer. The measurements of total hardness, oil and grease contents were performed in the SITEX Company.

3. Results and discussion

3.1. Catalyst characterization

3.1.1. Chemical composition characteristics

It can be seen in Table 1 that the iron amount in synthesized materials increased with increasing Fe/Al molar ratio. Also, Al amount increased slightly and achieved a maximum at Fe/Al molar ratio equal to 0.1 and then decreased at a molar ratio equal to 1which contents the highest quantity of iron. This could be the effect of aluminum dissolution or also is due to isomorphic substitution of aluminum by iron at the octahedral lattice [25].

3.1.2. Structural and morphological properties

Results are shown in Fig.1. The signal d_{001} of Na-bent shifts to the higher values in range of 19.36 Å and 14.49 Å indicating that the modification carried out over the clay leads, in all the cases, to the successful pillaring of the material. This peak was broadened and its intensity weakened by the incorporation of Fe-Al complexes, indicating that the Fe-Al complexes were intercalated randomly into the interlayer of bentonite [26]. The d_{001} values were clearly much greater at a relative small Fe/Al ratio, while these decreased to 14.49 Å at Fe/Al = 1, similar to previous results in which an increase of the Fe content produced materials with little increase in the basal spacing [27–29].

Pillaring phenomena was also confirmed by TEM analysis as shown in Fig. 2 for TEM micro graphs of the Na-bentonite and $FeAl_{0.1}$-bent, where the layer was kept and the basal spacing between two neighboring fringes was discarded, corresponding to the successful pillaring.

3.1.3. Surface area and porosities

The isotherms of N_2 adsorption of all synthesized pillared bentonites at 77 K were reported in our previous work [30], and to avoid similarity in this work it is given only isotherm of $FeAl_{0.1}$-bent and Na-bent in Fig. 3. According to the IUPAC classification, isotherms are of IV type with a well defined H_4 hysteresis loop, denoting a slit-shaped porosity between plate like particles. The modified samples had much similar total pore volume (V_t) compared to the Na-bentonite (Table 2). The negative effect on the textural properties of FeAl-bents induced by excessive iron content was also observed in terms of the specific surface area, S_{BET}, where intercalation of the Na-bentonite with Fe/Al molar ratios > 0.01 gave smaller specific surface areas. It can be concluded that the introduction of Fe onto the material in high amount reduces the surface area that is due to the blocking of part of the catalyst pores. The micro pore area (S_{micr}) increased from 16.058 m^2/g for Na-bent to 20.112 m^2/g for $FeAl_{0.01}$-bent confirming the formation of micro pores due to the pillaring process. However, it decreased from $FeAl_{0.01}$-bent to $FeAl_1$-bent, where was found to be 0m^2/g. This larger

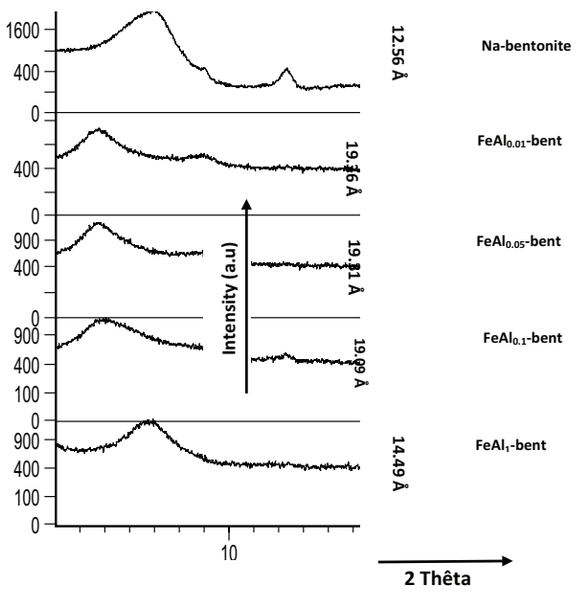

Fig. 1. X-ray diffraction spectra of raw and pillared bentonites.

Table 1
Characterization of Na-bentonite and pillared bentonite

Samples	CEC	SiO_2	Al_2O_3	Fe_2O_3	MgO	CaO	Na_2O	K_2O
Na-bentonite	71.93	55.21	20.09	7.10	3.33	0.13	1.97	0.29
$FeAl_{0.01}$-bent	24	53.08	27.32	9.36	2.94	0.088	0.23	0.21
$FeAl_{0.05}$-bent	21.33	52.14	28.23	10.68	2.93	0.09	0.21	1.16
$FeAl_{0.1}$-bent	17.33	52.00	28.87	12.19	2.84	0.097	0.18	1.02
$FeAl_1$-bent	12.33	53.34	20.14	18.28	2.44	0.10	0.19	1.10

CEC (meq/100 g): cation exchange capacity

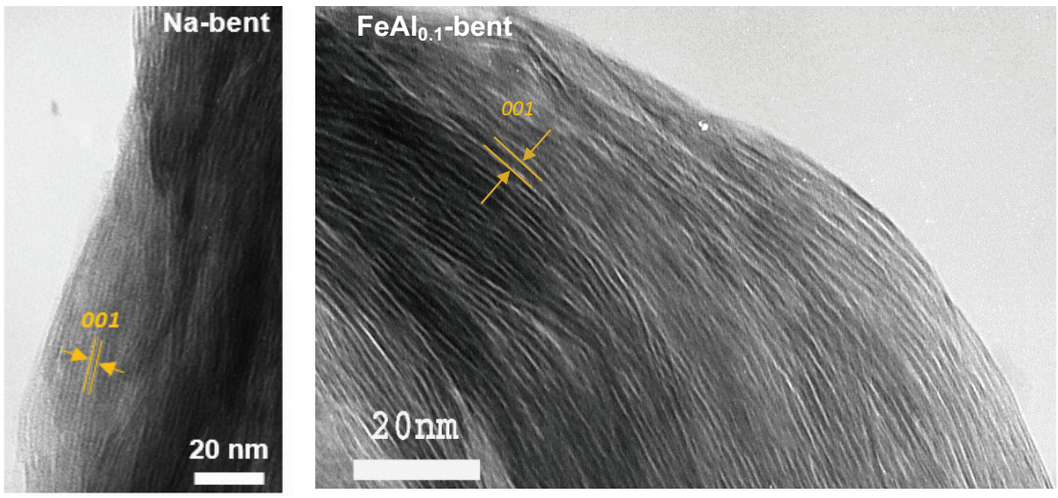

Fig. 2. Morphology of Na-bent and $FeAl_{0.1}$-bent at different scale given by TEM.

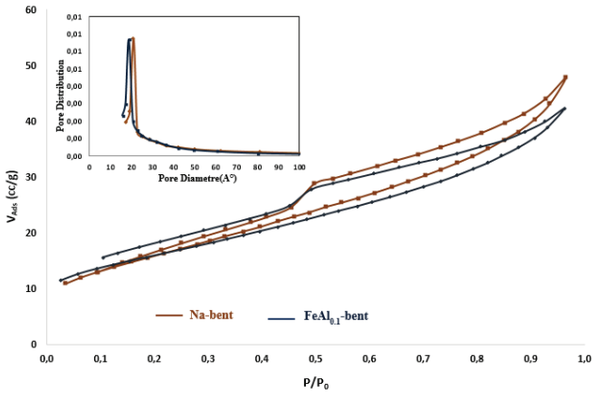

Fig. 3. Adsorption-desorption isotherms of the $FeAl_{0.1}$-bent and Na-bent from nitrogen sorption data (Inside: pore size distribution of both samples: $FeAl_{0.1}$-bent and Na-bent).

decrease for the micro pore area vs. the total surface area indicated that majority of new surface areas created in the pillaring process with iron species corresponded to meso pores (S_{mesop} increased from 38.316 m^2/g to 44.278 m^2/g for Na-bent and $FeAl_1$-bent, respectively). This was usually attributed to iron species adsorbed on the external surface of the catalyst leading to spatial arrangement with pore formation of different sizes in the micro- and meso-pore regions [31,32]. The meso pores resulted from interparticle spaces generated by three-dimensional coaggregation of iron polyoxocations on the clay mineral surface forming delaminated structures, whereas micro pores arose from intercalation of smaller hydrolyzed iron oxides and from micro porous interstices existing among the iron aggregates and clay minerals layers [33].

The pore size distributions of Na-bent and FeAl-PILC were obtained by applying BJH method to the desorption branch of the N_2 isotherms. Inside Fig. 3 compares the change of pore size distribution for the Na-bent and synthesized $FeAl_{0.1}$-bent samples. As can be seen, there is a good agreement between the pore sizes distributions of the samples studied.

3.1.4. Optical properties

It can be seen from Fig. 4A that, Na-bentonite presented UV-light absorption only, however, the synthesized FeAl-bents exhibited adsorption in the visible light region. After the introduction of iron on framework of natural bentonite, almost all catalysts showed prominent absorbance in the visible light region, and the visible light absorption abilities of materials were gradually increased with the increase of loaded-iron content. These results indicated strongly that the optical properties of bentonite could be extended to the visible light region by pillaring process with Fe and Al polycations. This confirms the activity of studied catalyst under UV and visible lights.

As shown in Fig. 4B, the PL emission maxima of all pillared bentonites are at 534 nm for all catalysts and only $FeAl_1$-bent present the lowest PL emission intensity. This is can be explained by the increasing of iron load that can allow the decrease of PL intensity. The same results were reported by Ping et al. [34], the photoluminescence analysis of Fe doped $SrTiO_3$ shows a decrease in PL intensity with increasing the iron concentration. In their study, Ping et al. [34] explains this phenomenon as follows: the iron incorporated into the $SrTiO_3$ can act as the electron-trapped agent to promote the electron-hole separation at low iron load, while as the recombination center when the iron concentration exceeds the threshold and begins to aggregate.

3.1.5. Cationic exchange capacity

The cation exchange capacity (CEC) of Na-bentonite and mixed pillared bentonite was determined using the copper ethylendiamine ($(EDA)_2CuCl_2$) complex. Results (Table 1) show that the CEC decreases with the increase of Fe/Al ratio, it shifts from 71.93 meq/100 g (Na-bentonite)

Table 2
Textural parameters of the samples (surface area and porosities)

Samples	S_{BET} (m^2/g)	$S_{BJH/mesp}$ (m^2/g)	V_{ads} (cm^2/g)	$V_{BJH/mesp}$ (cm^2/g)	S_{ext} (m^2/g)	S_{micr} (m^2/g)	V_{micr} (cm^2/g)	D(Å)
Na-bent	57.963	38.316	0.07	0.059	41.905	16.058	0.008	19.109
$FeAl_{0.01}$-bent	61.673	34.706	0.08	0.063	41.560	20.112	0.011	18.848
$FeAl_{0.05}$-bent	55.429	30.856	0.07	0.046	36.114	19.315	0.01	18.904
$FeAl_{0.1}$-bent	50.086	30.069	0.05	0.047	29.036	0	0	19.003
$FeAl_1$-bent	53.854	44.278	0.09	0.078	53.854	0	0	18.848

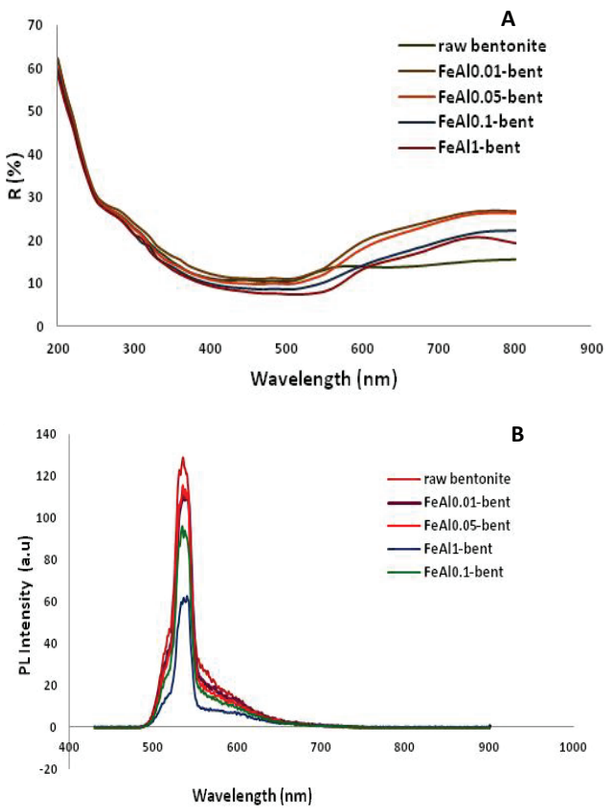

Fig. 4. (A) UV-Vis diffuse reflection spectra of catalyst and (B) PL spectra of different samples at an excitation wavelength of 400 nm

to 12.33 meq/100 g ($FeAl_1$-bent). These results confirm the reality of the insertion of the pillars into the bentonite.

3.2. Factorial effects of the heterogeneous Fenton-like degradation

3.2.1. Effect of initial pH

The pH value of the dye solution is a key parameter for catalytic degradation of dye because the adsorption of pollutants on the surface of catalysts is affected by it. Furthermore, formation of hydroxyl radical in the dye solution is dependent on pH, so adjusting pH is one of the most important parameters in the degradation process. To estimate effect of pH on the oxidation process, the reaction was carried out at different pH values (pH 3, 8 and 11) using HCl and/or NaOH (0.1 M) as pH adjustment chemicals. Initial pH of the dye solution was effective at neutral pH and at pH 3, the removal rate was the highest (Fig. 5A), but at pH 11 the removal rate was the lowest. In order to understand the effect of pH on the oxidation reaction, the role of pH on adsorption process must be explained. The surface change of $FeAl_{0.1}$-bent was determined by mass titration and results show that the surface charge of catalyst is positive in acidic pH, which decreases gradually with an increase of pH and passes through zero potential at pH 3.9. In an acidic pH range, the surface charge of the adsorbent increases mainly due to increased protonation of the silanol group. Congo red is an acidic dye and contains a negatively charged sulfonated group ($SO_3^-Na^+$). So, higher adsorption of the dye at lower pH is probably due to the increase in electrostatic attraction between the negatively charged dye molecules and positively charged catalyst surface.

3.2.2. Effect of initial concentration of H_2O_2 on Fenton process

The effect of H_2O_2concentration (i.e. 10, 20 and 48.5 $mmol{\cdot}L^{-1}$) on the degradation process of CR molecules in three experiments is shown in Fig. 5B by representing the dependence of discoloration process rate on the concentration of H_2O_2, while the catalyst dose (0.1 g/100 ml), pH 3, and temperature (25°C) were maintained constant. By increasing the concentration of H_2O_2, the rate of catalytic process increased too. As it is presented in Fig. 5B, after 20 min the CR dye degradation by Fenton oxidation dye increased at a faster rate from 68.55% to 88.52% when the molar concentration of H_2O_2 increased from 10 to 48.5 $mmol{\cdot}L^{-1}$, and then at slower rates afterwards. This result is due to the fact that by increasing H_2O_2 initial concentrations, concentration of $HO^{\bullet}$ radical in the process was increased too and so enhancement in the rate of dye degradation process took place. Thus for further experiments, the optimum concentrations of H_2O_2 was attained at 48.5 $mmol{\cdot}L^{-1}$.

3.2.3. Effect of catalyst load

To investigate the role of catalyst load on the catalytic-oxidation process, three experiments (0.05, 0.1 and 1.5 g/100 ml) were carried out while all other conditions were constant. In the absence of catalyst, there is no evidence

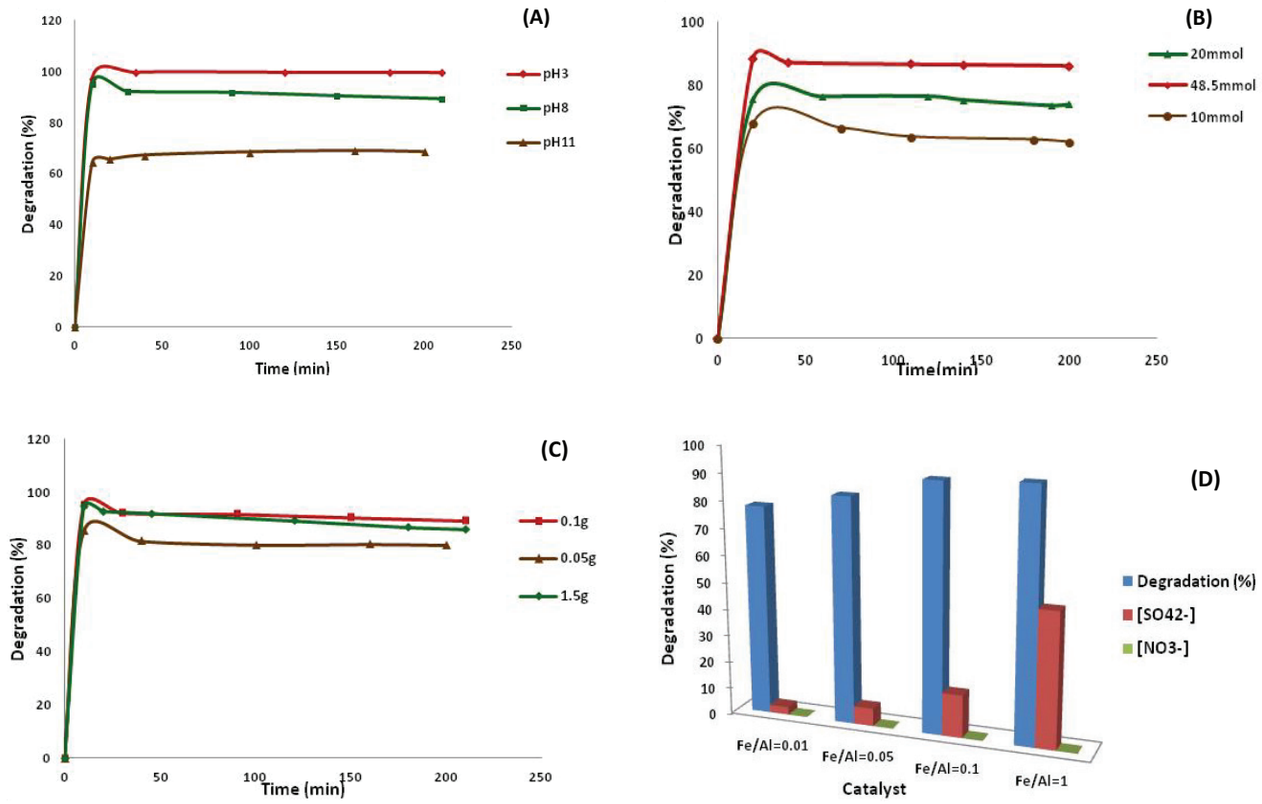

Fig. 5 (A) Effect of initial pH for dye degradation(Test conditions: $5{\cdot}10^{-4}$ mol·L^{-1} dye concentration, 25°C and 0.1 g of catalyst per 100 ml and 48.5 mmol H_2O_2) (B) The influence of catalyst masses (Test conditions: $5{\cdot}10^{-4}$ mol·L^{-1} dye concentration, pH = 3, 25°C and 48.5 mmol H_2O_2) and (C) The effect of H_2O_2 dosage for dye degradation (Test conditions: $5{\cdot}10^{-4}$ mol·L^{-1} dye concentration, pH = 3, 25°C and 0.1 g of catalyst) and (D) Effect of iron load on dye mineralization: [SO_4^{2-}] and [NO_3^-] (Test conditions: $5{\cdot}10^{-4}$ mol·L^{-1} dye concentration, 48.5 mmol H_2O_2, 25°C and 0.1 g of catalyst per 100 ml of sample).

of Fenton oxidation reaction when, for instance, hydrogen peroxide is added to a CR solution. As the catalyst load is increased, the rate of CR degradation accelerates. Further, for the catalyst load of 0.1 and 0.5 g/100 ml, the degradation of dye is almost the same after certain reaction time (Fig. 5C). The reason for this finding might be that by increasing catalyst amount above 0.1 g/100 ml, the numbers of $FeAl_{0.1}$-bent accessible active sites decrease because of catalyst particle aggregation and so additional catalyst is not involved in the catalytic activity [35]. Similar observations have been reported by other researchers; Wei et al. [36] investigated the effect of iron pillared montmorillonite (Fe-Mt) concentration on phenol photo-Fenton degradation in the range from 0.6 to 4 g/L. Results shows an increase in % removal with an increase in Fe-Mt up to 3 g/L, but it decreased upon further addition of Fe-Mt to 4 g/L. For our work,only 0.1 g/100 ml has been taken as selected catalyst amount.

It's well remarkable in Fig. 5 A, B and C, who presented the degradation rate (%) of CR dye versus reaction time (min), as lightly decrease of % degradation after reaching its maximum value and increase again to remain constant until the end of reaction,in all three cases studied. This can be explained by slightly desorption of CR dye from catalyst surface.

3.2.4. Effect of the iron amount in the catalyst

In this section, the effect of Fe/Al ratio on dye degradation has been studied using 0.1 g·L^{-1} of catalyst. The absorbance measurement conducted by UV-vis spectrophotometer indicates the increase of discoloration from 80% to 94% with increase in iron load from 0.01 to 1/100 ml. Also, the mineralization of Congo red was measured by ion chromatography analysis. Then, results indicated that after 4 h of treatment all catalysts gave a major loss of initial Nas volatile N-compounds or NH_4^+ and allows the partial release of initial S as SO_4^{2-} ion, since some intermediates with lateral sulfonic groups are not destroyed. Table 3 and Fig. 5D show the quantification of NO_3^- and SO_4^{2-} ions for each catalyst. It can be seen that the catalyst $FeAl_1$-bent presents the highest catalytic activity and it was selected as optimum dose for Fenton-like oxidation of Congo red dye.

3.3. Evaluation of photo catalytic performance

Photo catalytic activities of FeAl-bents were evaluated on the degradation of Congo red. 150 mL of dye solution with $5{\cdot}10^{-4}$ M mixed with 0.1 g of photo catalyst $AlFe_1$-bent at pH 8. This mixture was stirred in the dark for 40 min to reach adsorption-desorption equilibrium of dye onto the

Table 3
The quantification of NO_3^- and SO_4^{2-} ions

Catalyst	$\%NO_3^-$	$\%SO_4^{2-}$
$FeAl_{0.01}$-bent	0	2.83
$FeAl_{0.05}$-bent	0.013	6.59
$FeAl_{0.1}$-bent	0.04	15.82
$FeAl_1$-bent	0.06	49.79

photo catalyst surface. Then, 48.5 mM of $H_2O_2$was added and the lamp was turn on. The Fig. 6(A) shows the photo degradation of CR by different ways under UV light irradiations. When no photo catalyst was added, the self decomposition of CR can almost be negligible. $FeAl_1$-bent presented poor photo catalytic activity after 120 min of UV light irradiation without H_2O_2, whereas it exhibited a prominent degrade efficiency with H_2O_2, also photolysis of H_2O_2 exhibited a good discoloration ratio and a 50% of dye mineralization to inorganic ions.

To quantify the degradation rate of samples, a pseudo-first order kinetic model was used to fit the degradation data using Ln $(C_0/C) = k_t + a$, where k is the reaction rate constant. Fig. 6B revealed the plot of Ln (C_0/C), and reaction time (t) is approximately linear, indicating the photo catalytic degradation process of CR followed the first-order kinetic model. The kinetic parameters of all reactions were calculated and listed in the inset of Fig. 6B, which also revealed that the heterogeneous Fenton reaction under UV light irradiation possessed the best photo degradation activity with a k value of 0.0417 min^{-1} compared with the k value of the photolysis of H_2O_2 (0.0271 min^{-1}), $AlFe_1$-bentunder UV light (0.0138 min^{-1}) and CR alone (0.0009 min^{-1}). These findings strongly confirmed the enhanced photo catalytic behavior of $FeAl_1$-bent photo catalyst.

3.4. Comparison of fenton and photo-fenton processes

Catalytic efficiency of synthesized Fenton-like catalysts was compared in Fenton-like oxidation process and photo-Fenton process for degradation of CRdye. Interestingly, the results summarized as below: The Fenton process, conducted in the presence of a catalyst and H_2O_2 in the dark, showed a notable change in terms of discoloration of Congo red 93% and achieved a mineralization efficiency of 50% after 240 min. As UV-visible light was applied to the Fenton reaction, the mineralization efficiency improved to 97% after 60 min. The photo-Fenton catalytic activity of the intercalated clay was, therefore, attributed to its potential to utilize UV-visible light.

Furthermore, the photo-Fenton progress method not only present high dye removal efficiency and catalytic activity but also needs more economic consumption in wastewater treatment from different points of view, especially time and cost. Even so, the major advantage of photo-Fenton is that hydroxyl radicals are generated into the reaction system by photolysis of H_2O_2under UV irradiations and the photo catalytic activity of heterogeneous catalysts FeAl-bents under UV-visible light. This has overcome the need to handle a large time and product. Also, this may be convenient for industrial use.

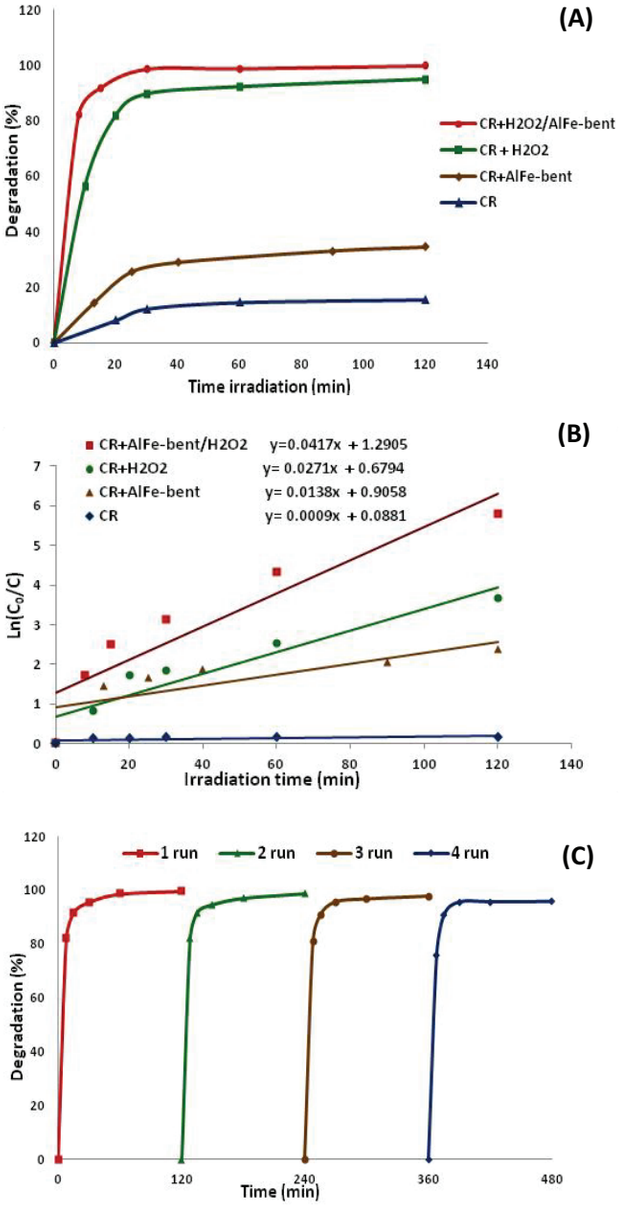

Fig. 6. (A) photo catalytic activity of CR under UV light irradiations, (B) Kinetics of the CR degradation over different samples, and (C) Cyclic photo degradation of CR by $FeAl_1$-bent.

3.5. Photo catalytic degradation of a real wastewater

Photo catalysts were also tested in the degradation of a real wastewater effluent sampled in the output of a wastewater textile company(SARTEX) located in the eastern of Tunisia.

According to results obtained on CRdye, it was chosen to study the degradation under UV irradiations and with only $FeAl_1$-bent of the textile effluent. Table 4 shows the most characteristics of the textile effluent before and after 3 h of treatment with heterogeneous Fenton reaction under ultraviolet irradiations. It can be seen from Table 4

that the photo catalytic activity of the prepared modified catalysts varied in the same order related to the degradation of CR dye. But,the degradation rate of textile wastewater was lower than that for CR dye. This could be explained by the fact that the effluent contained a mixture of organic compounds. The TOC measurements after photo catalytic treatment under UV irradiation clearly indicate the highest activity of FeAl pillared bentonite. The degradation of wastewater achieved by $FeAl_1$-bent was almost total after 3 h under UV irradiation. Even if the required time is longer, the use of UV light allows achieving almost a complete degradation of the organic compounds present in the wastewater sample (94%). Regarding their optical properties, this catalyst could be used for photo catalytic wastewater treatment under solar irradiation, leading to a cheap technology for developing countries.

Table 4
Most characteristics of real wastewater before and after photo-Fenton treatment

Quality indicators, mg/L	Initial textile effluent	Treated wastewater
pH	10	8
TOC	10	0.6
BOD5	600	90
COD	1400	200
Colour	3500	190
Suspended solids	200	2
Total Hardness	100	0.3
Oil and Grease	10	0.04
TDS	3500	2500
Chloride	1700	600

Table 5
Stability of catalyst at different cycles

Cycling	Degradation (%)	Leaching [Fe^{3+}](mg/L)
1	99.69	3.08
2	98.45	3.18
3	97.35	3.67
4	95.34	4.75

3.6. Stability of catalyst

The stability is a completely important characteristic for the catalyst when it is used in industrial application. It was evaluated by the adding of fresh dye solution in the treated effluent with 'spent' catalyst from the preceding run. On this system, the sample becomes reused over 4 times and its photo-Fenton activities were evaluated by measuring the % degradation of dye solution. As shown in Fig. 6C, the catalyst can preserve catalytic activities in the multiple runs and there is no remarquable loss of the activity throughout the whole reaction system. It indicates that the activity of the prepared sample is very stable. However, there is still a problem that whether the $OH^{\cdot}$ radicals come from the heterogeneous photo-Fenton reaction or from the homogeneous photo-Fenton reaction are owing to the iron ion leaching problem from the catalyst. The concentration of iron ions in the suspension was detected by SAA in this study. It should be noticed (Table 5) that the iron ion concentration comes to 3.08 ppm after 120 min of irradiation. The above results indicate that the iron ion amount leaching from the $FeAl_1$-bent catalyst is negligible.

These results confirm that the catalyst is chemically stable in the multiple photo-Fenton runs.

In this section, an overview of the published literature regarding the application of photo-Fenton's process for the degradation of organic dye is presented. Table 6 compares the results performed in terms of discoloration and mineralization efficiency,in the presence of the pillared clay presented in this work, to other previously published results, considering photo-Fenton process in the presence of different catalysts.

It can be seen from Table 6, a high influence on the catalyst type and dye is remarked. Each catalytic system acts differently and achieves its maximal degradation in case of polluting dye, and cannot be extrapolated from one system

Table 6
Comparison of catalytic efficiencies and time for different catalysts

Catalyst	Dye	Discoloration(%) = X Mineralization(%) = Y	References
Fe-Montmorillonite	Methylene Blue	X = 93 (t =180 min)	[39]
Fe-Montmorillonite	Reactive Brillant Orange X-GN	X = 98.6% y = 52.9% (t = 140 min)	[37]
Iron-zeolithe	Congo Red	X = 100% (t = 4 h)	[40]
AlFe-bentonite	Congo Red	X = 100% (t = 20 min) y = 100% (t = 60 min)	This work
Iron-carbon fibers	Congo Red	X = 100% (t = 80 min)	[41]
Fe-bentonite	Azo dye Orange II	X = 100% (t =60 min)	[42]
Fe-Laponite	Reactive Red HE-3B	X = 100% (t = 30 min) y = 76% (t = 120 min)	[38]
Iron-collagen fiber	Malachite Green (MG)	X = 100% (t = 30 min)	[43]

to another. However, some comments can be noted: a total mineralization was reached only in 60 min compared to other study such as Chen et al. [37] who obtain only 52.9% in 140 min and Feng et al. [38] who obtained 76% in 120 min. Also, in term of discoloration in our case we reached 100% in short time (only 30 min) compared to the above mentioned works.

So, from our point of view, to establish a reliable process for a real application in the textile industry, it is necessary to consider cost, time and efficiency.

4. Conclusions

In this work, heterogeneous catalysts with many properties were obtained through a simple, inexpensive and innovative route. The developed material is pillared bentonite with mixed Al-Fe pillars between the clay layers.

The micropourous materials were characterized by XRD, BET and UV-visible techniques in reflectance diffuse. XR diffraction showed an increase in the basal spacing up to 19 Å. They have a high thermal stability. Textural characterization shows a decrease in BET surface area indicating that a portion of iron was inserted into the clay structure being deposited on the surface, interacting with the tetrahedral sheets of the clay, without destroying the original framework.

Different parameters that affected in degradation of CR dye by using as catalyst the prepared FeAl-bent were found to achieve the best condition.

Results show that the optimized parameters are temperature 25°C, initial pH= 3, 48.5mmolinitial concentration of H_2O_2 and 0.1 g/100 ml catalyst load.

The photo catalytic activity of as synthesized samples was examined by photo catalytic degradation of Congo red and of real textile wastewater under UV-visible light irradiations. Above-mentioned discussions it is indicated that the prepared catalyst exhibits good photo catalytic activities both on degradation and mineralization of dye and real wastewater solutions. Finally, it was found that the synthesized heterogeneous catalysts were chemically stable and catalyst can be regenerated and reused for at least three times without significant loss of activity.

Photo-Fenton was considered as a preferable method for degradation of different kinds of wastewater.

References

[1] G. Ghasemzadeh, M. Momenpour, F. Omidi, M.R. Hosseini, M. Ahani, A. Barzegari,Applications of nano materials in water treatment and environmental remediation, Front Environ Sci Eng., 8(4) (2014) 471–482.
[2] H. Chaker, L. Chérif-Aouali, S. Khaoulani, A. Bengueddach, S. Fourmentin, Photo catalytic degradation of methyl orange and real wastewater by silver doped mesoporous TiO_2 catalysts, J. Photoch Photobio A: Chem., 318 (2016)142–149.
[3] M. Khadhraoui, H. Trabelsi, M. Ksibi, S. Bouguerra, B. Elleuch,-Discoloration and detoxicification of a Congo red dye solution by means of ozone treatment for a possible water reuse, J Hazard. Mater., 161(2) (2009) 974–981.
[4] C. Srilakshmi, R. Saraf, Ag-doped hydroxyapatite as efficient adsorbent for removal of Congo red dye from aqueous solution: Synthesis, kinetic and equilibrium adsorption isotherm analysis, Micropor. Mesopor. Mater., 219 (2016) 134–144.
[5] I.M. Banat, P. Nigam, D. Singh, R. Marchant, Microbial decolorization of textile-dye containing effluents: a review, Bioresour. Tecnol., 58(3) (1996) 217–227.
[6] N.Al-Bastaki, Removal of methyl orange dye and Na_2SO_4 salt from synthetic waste water using reverse osmosis, Chem Eng Proces: Process Intensif., 43(12) (2004)1561–1567.
[7] V. Golob, A. Vinder, M. Simonič, Efficiency of the coagulation/flocculation method for the treatment of dye bath effluents, Dyes Pigm., 67(2) (2005) 93–97.
[8] M. Tekbaş, H.C. Yatmaz, N. Bektaş, Heterogeneous photo-Fenton oxidation of reactive azo dye solutions using iron exchanged zeolite as a catalyst, Micropor. Mesopor. Mater., 115(3) (2008) 594–602.
[9] S. Irmak, H.I. Yavuz, O. Erbatur, Degradation of 4-chloro-2-methylphenol in aqueous solution by electro-Fenton and photoelectro-Fenton processes,Appl. Catal. B: Environ., 63(3) (2006) 243–248.
[10] E. Brillas, I. Sirés, M.A. Oturan,Electro-Fenton process and related electrochemical technologies based on Fenton's reaction chemistry, Chem Rev., 109(12) (2009) 6570–6631.
[11] B. Boye, M.M. Dieng, E. Brillas, Degradation of herbicide 4-chlorophenoxyacetic acid by advanced electrochemical oxidation methods, Environ. Sci Tech., 36(13) (2002) 3030–3035.
[12] X. Zhu, B.E. Logan, Using single-chamber microbial fuel cells as renewable power sources of electro-Fenton reactors for organic pollutant treatment, J. Hazard. Mater., 252 (2013) 198–203.
[13] C. Hsueh, Y. Huang, C. Wang, C-Y. Chen, Degradation of azo dyes using low iron concentration of Fenton and Fenton-like system, Chemosphere., 58(10) (2005) 1409–1414.
[14] H. Zhang, D. Zhang, J. Zhou, Removal of COD from landfill leachate by electro-Fenton method, J Hazard. Mater., 135(1) (2006) 106-111.
[15] Y. Yuan, B. Zhao, S. Zhou, S. Zhong, L. Zhuang, Electro catalytic activity of anodic biofilm responses to pH changes in microbial fuel cells, Bioresour. Tecnol., 102(13) (2011) 6887–6891.
[16] J. Herney-Ramirez, M.A. Vicente, L.M. Madeira, Heterogeneous photo-Fenton oxidation with pillared clay-based catalysts for wastewater treatment: a review, Appl. Catal. B: Environ., 98(1) (2010) 10–26.
[17] J. Chen, L. Zhu, Heterogeneous UV-Fenton catalytic degradation of dyestuff in water with hydroxyl-Fe pillared bentonite, Catal. Today, 126(3) (2007) 463–470.
[18] Y. Gao, Y. Wang, H. Zhang, Removal of Rhodamine B with Fe-supported bentonite as heterogeneous photo-Fenton catalyst under visible irradiation,Appl. Catal. B: Environ., 178 (2015) 29–36.
[19] M.F. Hou, C.X. Ma, W.D. Zhang, X.Y. Tang, Y.N.Fan, H.F.Wan,Removal of rhodamine B using iron-pillared bentonite, J. Hazard. Mater., 186(2) (2011) 1118–1123.
[20] R.S. Jack, G.A. Ayoko, M.O. Adebajo, R.L. Frost, A review of iron species for visible-light photo catalytic water purification, Environ. Sci. Pollut. Res., 22(10) (2015) 7439–7449.
[21] M. Neamtu, A. Yediler, I. Siminiceanu, A. Kettrup, Oxidation of commercial reactive azo dye aqueous solutions by the photo-Fenton and Fenton-like processes, J. Photochem. Photobiol. A: Chem., 161(1) (2003) 87–93.
[22] U. Pagga, D. Brown, The degradation of dyestuffs: Part II Behaviour of dyestuffs in aerobic biodegradation tests, Chemosphere, 15(4) (1986) 479–491.
[23] S. Chinwetkitvanich, M. Tuntoolvest, T. Panswad, Anaerobic decolorization of reactive dye bath effluents by a two-stage UASB system with tapioca as a co-substrate, Water Res., 34(8) (2000) 2223–2232.
[24] S. Khelifi, F. Ayari, D. Hassan Chehimi, M. Trabelsi-Ayadi, Synthesis and characterization of heterogeneous catalysts and comparisonto iron-ore, J Chem Eng Proc Technol., 316(7) (2016). doi:10.4172/2157-7048.1000316
[25] A.A. Jara, S. Goldberg, M. Mora, Studies of the surface charge of amorphous alumino silicates using surface complexation models, J. Colloid Interf. Sci., 292(1) (2005) 160–170.

[26] S. Caudo, G. Centi, C. Genovese, S. Perathoner, Copper-and iron-pillared clay catalysts for the WHPCO of model and real wastewater streams from olive oil milling production, Appl. Catal. B: Environ., 70(1) (2007) 437–446.
[27] S. Letaïef, B. Casal, P. Aranda, M.A. Martín-Luengo, E. Ruiz-Hitzky, Fe-containing pillared clays as catalysts for phenol hydroxylation, Appl. Clay Sci., 22(6) (2003) 263–277.
[28] T. Undabeytia, M.C. Galán-Jiménez, E. Gómez-Pantoja, J. Vázquez, B. Casal, F. Bergaya, E. Morillo, Fe-pillared clay mineral-based formulations of imazaquin for reduced leaching in soil,Appl. Clay Sci., 80 (2013) 382–389.
[29] P.K. Mandali, D.K. Chand, Palladium nano particles catalyzed Suzuki cross-coupling reactions in ambient conditions, Catal. Commun., 31 (2013) 16–20.
[30] S. Khelifi, F. Ayari, A. Choukchou-Braham, D. Hassan Chehimi, The remarkable effect of Al–Fe pillaring on the adsorption and catalytic activity of natural Tunisian bentonite in the degradation of azo dye, J Por. Mater., (2017)1–12.
[31] T.J. Bandosz, K. Cheng, Changes in acidity of Fe-pillared/delaminated smectites on heat treatment,J. Colloid Interf. Sci., 191(2) (1997) 456–463.
[32] J.L. Marco-Brown, C.M. Barbosa-Lema, R.M.T. Sánchez, R.C.Mercader, M. dos Santos Afonso, Adsorption of picloram herbicide on iron oxide pillared montmorillonite. Appl. Clay Sci., 58 (2012) 25–33.
[33] P. Yuan, F.A. Bergaya, Q. Tao, M. Fan, Z. Liu, J. Zhu H. He, T. Chen, A combined study by XRD, FTIR, TG and HRTEM on the structure of delaminated Fe-intercalated/pillared clay, J. Colloid Interf. Sci., 324(1) (2008) 142–149.
[34] P. Li, C. Liu, G. Wu, Y. Heng, S. Lin, A. Ren, Lv. Kehan, X. Lisong, S. Weidong, Solvothermal synthesis and visible light-driven photo catalytic degradation for tetracycline of Fe-doped $SrTiO_3$, RSC Adv., 4(88) (2014) 47615–47624.
[35] Z.R. Lin, X.H. Ma, L. Zhao, Y.H. Dong, Kinetics and products of PCB28 degradation through a goethite-catalyzed Fenton-like reaction, Chemosphere, 101 (2014) 15–20.
[36] X. Wei, H. Wu, G. He, Y. Guan, Efficient degradation of phenol using iron-montmorillonite as a Fenton catalyst: Importance of visible light irradiation and intermediates, J. Hazard. Mater., 321 (2017) 408–416.
[37] Q. Chen, P. Wu, Y. Li, N. Zhu, Z. Dang, Heterogeneous photo-Fenton photo degradation of reactive brilliant orange X-GN over iron-pillared montmorillonite under visible irradiation, J. Hazard. Mater., 168(2) (2009) 901–908.
[38] J. Feng, X. Hu, P.L. Yue, H.Y. Zhu, G.Q. Lu, Discoloration and mineralization of Reactive Red HE-3B by heterogeneous photo-Fenton reaction, Water Res., 37(15) (2003) 3776–3784.
[39] M.A. De León, J. Castiglioni, J. Bussi, M. Sergio, Catalytic activity of an iron-pillared montmorillonitic clay mineral in heterogeneous photo-Fenton process, Catal. Today, 133 (2008) 600–605.
[40] J. Feng, X. Hu, P.L. Yue, H.Y. Zhu, G.Q. Lu, A novel laponite clay-based Fe nano composite and its photo-catalytic activity in photo-assisted degradation of Orange II, Chem. Eng. Sci., 58(3) (2003) 679–685.
[41] A. Gil, S.A. Korili, R. Trujillano, M.A. Vicente, Pillared clays and related catalysts, Springer., 2010.
[42] J. Feng, R.S. Wong, X. Hu, P.L. Yue, Discoloration and mineralization of Orange II by using Fe^{3+}-doped TiO_2 and bentonite clay-based Fe nano catalysts, Catal. Today, 98(3) (2004) 441–446.
[43] X. Liu, R. Tang, Q. He, X. Liao, B. Shi, Fe (III)-loaded collagen fiber as a heterogeneous catalyst for the photo-assisted decomposition of Malachite Green, J. Hazard. Mater., 174(1) (2010) 687–693.